Article ID: 1001-3555(2013)06-0530-09

Efficient Ru/AC Catalysts Prepared by Co-Impregnation for Ammonia Synthesis

NI Jun, ZHU Yong-long, CHEN Geng, LIN Jian-xin, WEI Ke-mei
(*National Engineering Research Center of Chemical Fertilizer Catalyst*, *Fuzhou University*, *Fuzhou* 350002, *China*)

Abstract: Ru+Ba+K/AC catalysts with high turnover frequency were synthesized by co-impregnation with $Ba(NO_3)_2$ and the complex compound of glycerol and K_2RuO_4. The turnover frequency of the prepared catalysts is between 0.87 and 1.30 s^{-1}, which is 1.26 to 1.88 times higher than that of the Ru/AC catalyst with $RuCl_3$ as a precursor for ammonia synthesis. The higher turnover frequency of the Ru+Ba+K/AC catalysts than the Ru/AC catalyst could be attributed to the higher absorption and lower activation energy of nitrogen on the Ru surface and the narrow-sized distribution of Ru nanocrystals at the reaction temperature.

Key words: Ruthenium; supported catalysts; heterogeneous catalysis; co-impregnation; turnover frequency
CLC number: O643.32 **Document code**: A

Ruthenium catalysts have been used in various catalytic reactions, such as in the isomerization of linoleic acid[1], the hydrogenolysis of glycerol[2-4], the selective hydrogenation of benzene, and the Fischer-Tropsch synthesis [5-7]. In the last decade, numerous studies examined the types of supports, promoters, and precursors of Ru compounds for ammonia synthesis[8-14]. However, the broad application of Ru catalysts is limited by their higher cost, more complex dechlorination preparation process, and poorer stability compared with fused iron catalysts. The small particle size and large specific surface area of the noble metal have been proposed to increase the catalytic efficiency of Ru catalysts. Heterogeneous catalysts without the well-defined mixture of particle sizes and surface shapes hamper the catalytic performance of Ru catalysts[15-16].

Among all precursors of Ru, $Ru_3(CO)_{12}$ is better than $RuCl_3$ based on high dispersion and security during ammonia synthesis. However, the high cost of the $Ru_3(CO)_{12}$ precursor obstructs the broad application of Ru catalysts for ammonia synthesis. Hence, $RuCl_3$ is widely used as a precursor of Ru because of its low cost. However, chlorine ion is very poisonous and needs to be removed through hydrogen reduction[17-18], hydrazine liquid reduction[19], or impregnation-precipitation[20]. The first method involves the use of H_2 and requires high temperature. This method usually results in uneven size, sintering of Ru nanoparticles (NPs), and methanation of carbon supports. The last method mentioned was developed to avoid several of the abovementioned adverse factors of hydrogen and hydrazine liquid reduction. The activity of the catalysts prepared through the impregnation-precipitation method is considerably higher than that of the catalysts obtained using the two other methods. The preparation process involves the reduction or elimination of chlorine ions, a substep in precursor impregnation, addition of agents, and the uneven dispersion of Ru NPs on the AC surface. These deficiencies could result in time-

Received date: 2013-10-07; **Revised date**: 2013-11-25.
Foundation: Technology Support Program of China (2007BAE08B02), Fujian Province Education Department Science and Technology project (JK2011005), and Natural Science Foundation of Fujian Province (2013J01038) and PetroChina Innovation Foundation (2013D-5006-0506).
First author: Jun Ni (1973-), male, assistant researcher.

consuming and inefficient preparation, low thermal stability, low turnover frequency (TOF), and potential hazard of chlorine ion residue in the equipment.

In this study, we describe a novel and convenient method to prepare a Ru+Ba+K/AC catalyst with high-TOF as well as high catalytic activity for ammonia synthesis. The catalyst was prepared by co-impregnating a Ru precursor and additivies, such as Ba and K. The Ru precursor was derived from the complexation of glycerol and K_2RuO_4, and the relatively affordable metal Ru powder and glycerol were used as the raw materials of the precursor. This process renders the dechlorination post-treatment, pre-reduction, substep impregnation of the precursor, and addition of additives unnecessary. Most Ru particles with well-defined facets are 3 to 5 nm in size. Thus, lower cost, simplified procedures for catalyst preparation, higher TOF, and catalytic activity for ammonia synthesis may be simultaneously achieved.

1 Experiment

1.1 Catalysts preparation

$RuCl_3$, ruthenium powder, KNO_3, KOH, $Ba(NO_3)_2$, and glycerol were used as base materials. Nitrate and glycerol were supplied by Sinopharm Chemical Reagent Co, LTD. $RuCl_3$ and ruthenium powder were supplied by Chenzhou Gaoxin Platinum Industry Co, LTD. All chemicals used in these experiments were of analytical reagent grade and were used without further treatment. The graphited activated carbon (denoted AC) was sieved to 1.70 ~ 1.18 mm particle size.

K_2RuO_4 was prepared by melting the mixture of ruthenium powder, KNO_3, and KOH with a molar ratio 1 ∶ 2 ∶ 5 in a nickel crucible at 600 ℃ for 1 h. K_2RuO_4 aqueous solution was then added into the glycerol aqueous solution with stirring to obtain a stable solution (denoted as Ru-GLY-K) that contains the Ru precursor (denoted as Ru-GLY). The molar ratio of Ru and glycerol is 1 ∶ 1. The concentration of Ru-GLY aqueous is about 1.4%.

The graphited AC was impregnated with the mixed solution of Ru-GLY-K, $Ba(NO_3)_2$ and HNO_3 at a pH of 1.0. The nominal contents of Ru and KOH in the AC were 4 and 16%, respectively. The nominal Ba loadings in the AC were 6.0%, 8.0%, 10.0%, and 12.0%. The Ru+Ba10+K/AC catalysis prepared by co-impregnating shows the contents of Ru, Ba and KOH were 4.0%, 10.0% and 16.0%, respectively. For comparison, the graphited activated carbon was impregnated with $RuCl_3$ in an aqueous solution. The promoters were introduced by impregnating a mixture solution of $Ba(NO_3)_2$ and KNO_3 after reducing $RuCl_3$ with hydrogen at 450 ℃ for 6 h and washing with deionized water at 70 ℃. The sample is referred to as Ru-Ba10-K/AC due to successively impregnating of Ru and promoters. The content of Ru, Ba and KOH were 4.0%, 10.0% and 16.0% for the Ru-Ba10-K/AC catalyst, respectively. The nominal contents of Ba and KOH promoters were 4% and 16%, respectively. All samples were evaporated and dried with an infrared light.

1.2 Characterization of Catalysts

The morphologies and particle sizes of Ru were studied using transmission electron microscopy (TEM, Tecnai G2F20 S-TWIN). Chemisorption was carried out using an Autochem 2 920 instrument (Micromeritics). Prior to measurement, the catalysts (ca. 100 mg) were reduced in H_2 at 500 ℃ for 1.5 h, and then flushed with helium for 2 h to remove H_2 that were adsorbed on the catalyst surface, followed by cooling to 50 ℃ in a helium stream. CO chemisorption was performed with pulse method by allowing CO to flow over the sample at a controlled temperature of 50 ℃. Ru dispersion was calculated from the cumulative volume of CO adsorbed during pulse, assuming a chemisorption stoichiometric ratio of CO/Ru = 1 ∶ 1.

The temperature-programmed desorption studies of pre-adsorbed nitrogen (N_2-TPD) and hydrogen (H_2-TPD) were performed in a glass-flow setup. Each sample was reduced in flowing hydrogen (50 mL/min). The sample was then flushed with argon at 500 ℃ (50 mL/min, 120 min) to remove the pre-adsorbed hydrogen. The reactor was cooled in room temperature with a cooling rate of 5 ℃/min, and the argon was replaced with hydrogen. Finally, the catalyst was flushed with argon (50 mL/min, 30 min), and the H_2-TPD experiment was performed. The concentration of hydrogen that desorbs to the Ar stream (50 mL/min) was monitored by TCD signal when the reactor was heated with a constant rate of 20 ℃/min. For N_2-TPD, the sample was flushed with helium at 500 ℃ (50 mL/min, 120 min) to remove the pre-adsorbed hydrogen. Helium was replaced with nitrogen, and the reactor was cooled in room temperature with a cooling rate of 5 ℃/min. Finally, the catalyst was flushed with helium (50 mL/min, 30 min), and the N_2-TPD experiment was performed. The concentration of nitrogen that desorbs to the He stream (50 ml/min) was monitored when the reactor was heated with a constant rate of 20 ℃/min.

The crystal structure was determined by powder X-ray diffraction (XRD, Philips, X′ Pert MPD, Co $K\alpha$, λ = 0.17889 nm). The component distribution was studied by energy dispersive spectrometry (EDS) using scanning electron microscopy (SEM, Hitachi 4 800). X-ray photoelectron spectroscopy (XPS) equipped with monochromatized AlKα X-ray radiation ($h\nu$ = 1 486.6 eV) (Thermo Fisher Scientific Co. ESCALAB 250, USA) was used to investigate the surface properties. The binding energy was corrected using the C 1s level at 284.6 eV as an internal standard.

1.3 Measurement of catalytic activity

Ammonia synthesis was carried out in a stainless steel reactor. About 2 mL of the catalysts with particle sizes of 1.70 ~ 1.18 mm were activated in a stoichiometric H_2 and N_2 mixture (200, 300, 400, 450, and 500 ℃ for 2 h, respectively) before testing, and then stabilized in the reaction conditions (such as, 10 MPa, 400 ℃, 10,000 h^{-1}, and H_2/N_2 = 3 : 1) for more than 2 h. The ammonia concentration in the effluent was determined by a chemical titration method [21].

2 Results and discussion

2.1 Size of the ruthenium nanoparticles

The structures of the Ru nano Crystals (NCs) from the Ru+Ba6+K/AC catalyst were confirmed by selected-area electron diffraction (SAED) and high-resolution transmission electron microscopy (HRTEM) (Fig. 1). The TEM images show that most Ru particles are 3 to 5 nm in diameter. Particles with diameters higher than 5 nm were also observed because of particle aggregation at a high temperature of 500 ℃. Some of the NPs for the Ru/AC catalyst based on $RuCl_3$ precursor are less than 2 nm in size, which is a disadvantage because supported Ru catalysts are structure sensitive during ammonia synthesis [12].

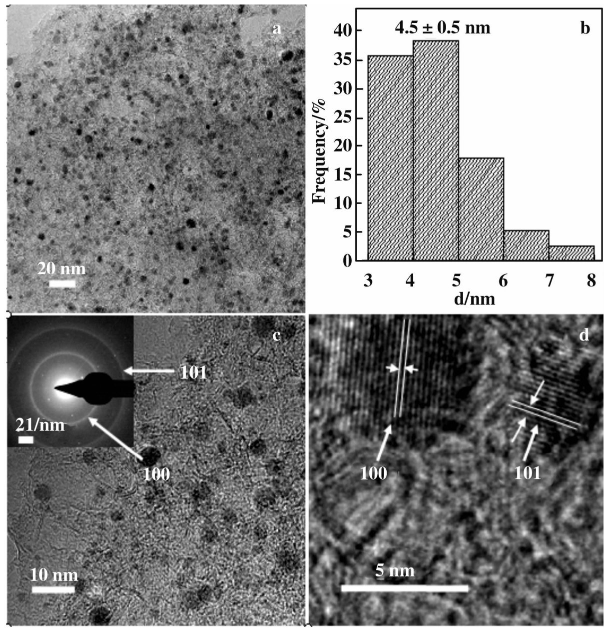

Fig. 1 (a) TEM images of Ru NPs from the Ru+Ba6+K/AC catalyst. (b) Size histogram of Ru NCs. (c) SAED pattern. (d) HRTEM image. Reduction conditions: 450 ℃ for 6 h

The TEM and HRTEM results show that the Ru particles from the two precursors possess different size distributions. The particles from the Ru-GLY precursor have well-defined facets and are more uniform. The HRTEM results show that Ru NPs predominantly expose the Ru atoms based on well-defined planes for the Ru+Ba6+K/AC catalyst by co-impregnation and that most NPs without well-defined planes are predominantly exposed for the Ru-Ba6-K/AC catalyst (Fig. 2). The reaction rate is remarkably sensitive to the catalyst surface structure[22]. Therefore, surface structure could be a key factor affecting the efficient synthesis of ammonia.

2.2 Temperature-programmed desorption of hydrogen (H_2-TPD) and temperature-programmed desorption of nitrogen (N_2-TPD)

The thermal desorption curves of hydrogen from

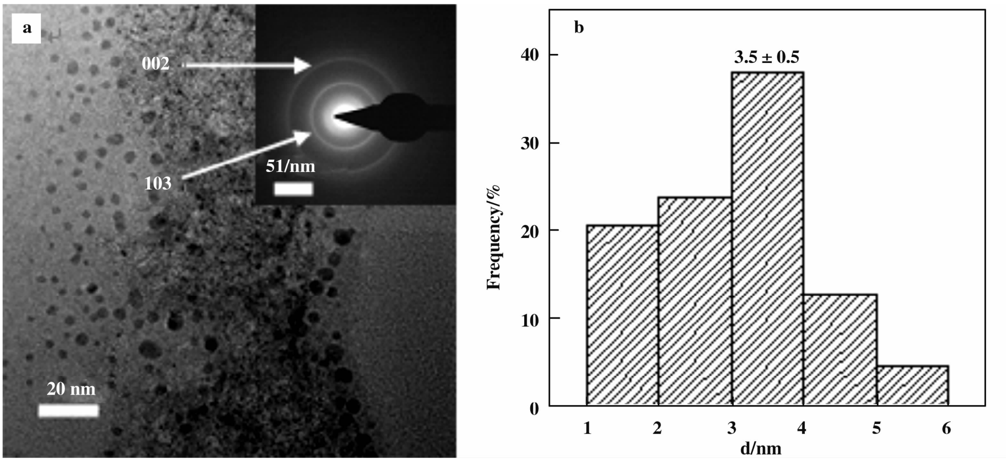

Fig. 2 (a) TEM images and SAED pattern of the Ru-Ba6-K/AC catalyst based on the $RuCl_3$ precursor. Reduction conditions: 450 ℃ for 6 h.

various samples are presented in Fig. 3 to understand the effect of preparation methods and different precursors on catalytic performance. The catalytic activity increases as the maximum peak temperature of H_2-TPD decreases. A low-temperature desorption peak for the Ru/AC catalysts is shown in Fig. 3. However, the novel desorption peak at a high temperature would increase because of the action of promoters. The desorption quantity of the Ru/AC catalysts promoted with Ba and K increases at low temperatures; thus, Ba and K are suggested to increase the adsorption of H_2. An increase in H_2 adsorption at low and high temperatures may be attributed to the enhanced electron density of Ru because of the charge transfer from Ba and K [23]. H_2 desorption at a temperature significantly higher than 400 ℃ could be unfavorable for the catalytic activity tested at 400 ℃ during ammonia synthesis. As shown in Fig. 3, H_2 desorption is easier for the Ru+Ba10+K/AC catalyst at either low or high desorption temperature. A lower desorption temperature leads to a higher catalytic activity during ammonia synthesis. This finding is consistent with related conclusions about the influence of H_2 chemisorption on the activity of ammonia synthesis [24]. The desorption peaks of the Ru+Ba10+K/AC and Ru-Ba10-K/AC catalysts are reached at 421 and 450 ℃, respectively. More adsorbed hydrogen molecules would occupy the active sites of the Ru surface and would inhibit the adsorption of nitrogen at the reaction condition for the Ru-Ba10-K/AC catalyst.

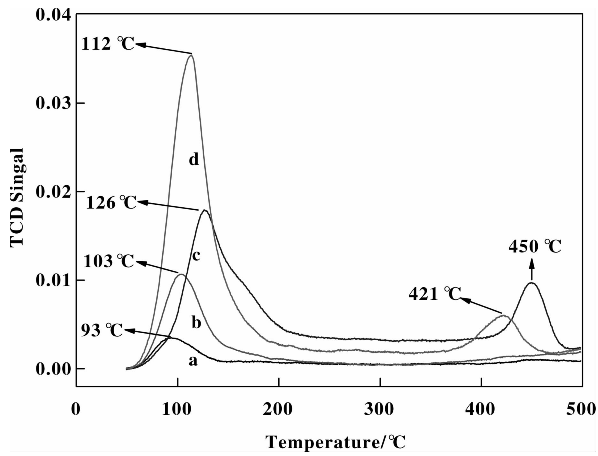

Fig. 3 H_2-TPD profiles of the catalysts

a. Ru/AC based on $RuCl_3$ precursor, b. Ru /AC based on Ru-GLY precursor, c. Ru-Ba10-K/AC, d. Ru+Ba10+K/AC

N_2 desorption is the inverse reaction of the rate-determining step of ammonia synthesis [25-27]. Therefore, the efficient dissociation of N_2 at the reaction conditions should be favorable during ammonia synthesis. As shown in Figs. 3 and 4, the nitrogen desorption of the catalysts prepared by the $RuCl_3$ precursor is weaker than that of the catalysts prepared by the Ru-GLY precursor at low temperatures. This result suggests that the nitrogen desorption of the Ru-Ba10-K/AC catalyst is signifiantly stronger at low temperatures. According to the results of N_2-TPD, the N_2 desorption quantity of the Ru-Ba10-K/AC catalyst is almost the same as that of the Ru+Ba10+K/AC catalyst at high temperatures. However, according to the results of H_2-TPD, hydrogen would occupy less adsorption sites at the reaction temperature for the Ru+Ba10+K/AC catalyst. These results suggest that more nitrogen molecules would be adsorbed on the Ru surface for the Ru+Ba10+K/AC catalyst at the reaction temperature.

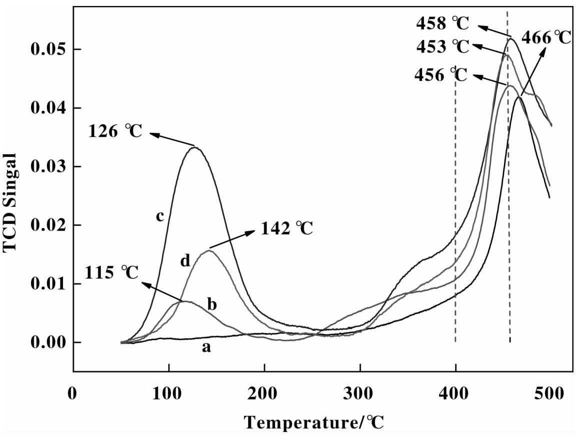

Fig. 4 N_2-TPD profiles of the catalysts

a. Ru/AC based on $RuCl_3$ precursor, b. Ru/AC based on Ru-GLY precursor, c. Ru-Ba10-K/AC, d. Ru+Ba10+K/AC

Conversely, the second desorption peak temperatures of N_2 are 466, 456, 458, and 453 ℃ for the Ru/AC catalyst based on the $RuCl_3$ precursor, Ru/AC catalyst based on the Ru-GLY precursor, Ru-Ba10-K/AC catalyst, and Ru+Ba10+K/AC catalyst, respectively. The desorption peak temperature of the Ru/AC catalyst based on the Ru-GLY precursor is lower than that of the the Ru/AC catalyst based on the $RuCl_3$ precursor. Nitrogen could be activated much easier for the catalyst via co-impregnation at the reaction temperature. The desorption peak temperature is also lower after loading the promoters with Ba and K for the Ru+Ba10+K/AC catalyst compared with the Ru-Ba10-K/AC catalyst. This result reveals that the novel approach decreases the activation energy of nitrogen desorption. The variation tendency of the activation energy of reaction and desorption is consistent. The decrease in activation energy indicates that the reaction rate of ammonia synthesis could be higher at the reaction conditions [28-29].

Combined with the H_2-TPD results, the increase in TOF may remarkably derive the alteration of adsorption and dissociation of H_2 and N_2 at the reaction temperature. The high TOF of ammonia synthesis could be a synergism of more adsorbance and lower activation energy of nitrogen at the reaction temperature for the Ru+Ba10+K/AC catalyst.

2.3 XRD

Figure 5 shows XRD patterns of the reduced catalysts. The main crystal phase is $BaCO_3$ (JCPDS 05-0378) without the diffraction maximum of Ru and K_2CO_3 for the Ru-Ba10-K/AC and Ru+Ba10+K/AC catalysts from different precursors and preparation methods. The $BaCO_3$ is a product of BaO or $Ba(OH)_2$ and CO_2 after the reduced catalysts exposed in air. The results show that the difference of small crystallites of Ba promoter is inapparent for the catalysts prepared by different methods. The grain size of Ba species is not the key factors influencing the catalyst performance.

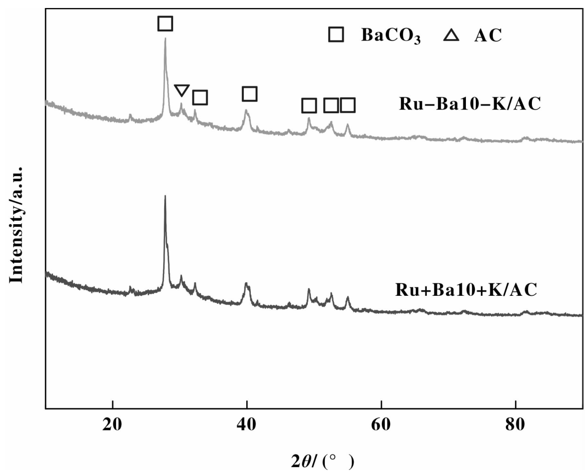

Fig. 5 XRD patterns of the catalysts

2.4 SEM-EDS

Figure 6 is EDS mapping of the reduced catalysts. These results show that the difference of distribution for ruthenium and the promoters on surface of two kinds of catalysts is little. This could be a result that most Ru and promoters enter into the pore canal of micropore and mesoporous. The distribution of Ru and promoters on the AC surface could be correlation with the surface groups of AC. The different of element distribition is indistinctive for the catalysts from different preparation methods based on the same support.

2.5 XPS

Figure 7 shows the XPS spectra of the Ru-Ba10-K/AC and Ru+Ba10+K/AC catalysts. In the Ru 3d XPS spectra, the Ba-K-Ru/AC catalyst presented one

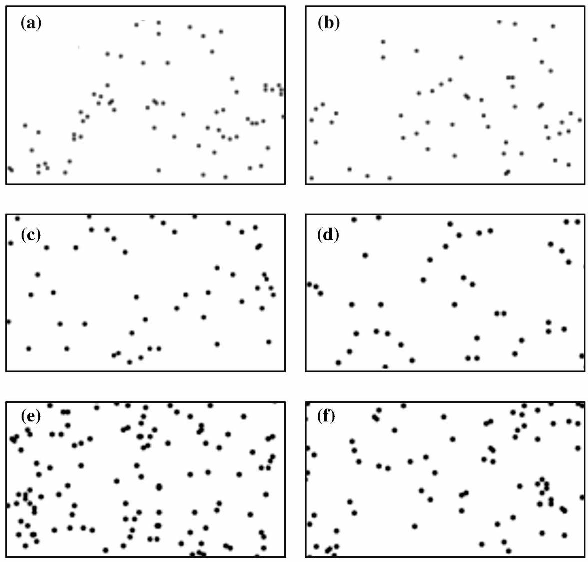

Fig. 6 EDS mapping of the catalysts after reducing with hydrogen (a)(c)(e): Ru-Ba10-K/AC, (b)(d)(f): Ru+Ba10+K/AC; (a)(b): Ru; (c)(d): Ba; (e)(f): K

strong peak at the binding energy of 281.7 eV, which corresponds to Ru^0 $3d_{5/2}$ [30]. In the Ba 3d XPS spectra, two peaks at ~777 and 780 eV were observed on the Ba-K-Ru/AC and La-Ba-K-Ru/AC catalysts. according to the literature [31- 32], the peak at ~780 eV can be attributed to Ba^{2+} $3d_{5/2}$, whereas the peak at ~777 eV may be assigned to low-valence Ba species. The presence of two states of Ba species is consistent with the literature[33-34]. It has been reported that a part of Ba can be reduced to BaOx with a low valence and then transferred onto the surface of Ru particles under the ammonia synthesis reaction [33]. More low valence BaO_x in the Ru-Ba10-K/AC catalyst suggest that the reduction degree of Ba is higher for the catalysts with the normal preparation method. However, more low valence BaO_x with a low melting point in catalyst is unfavorable to the stability of the catalyst.

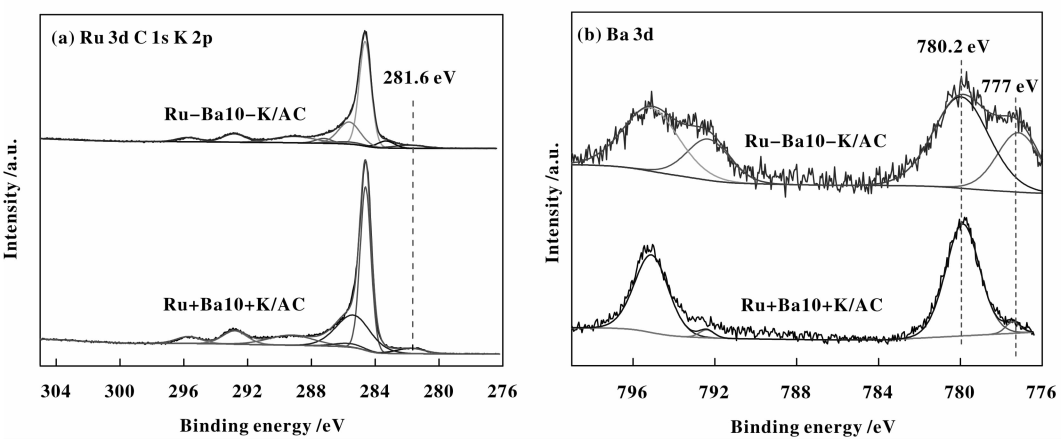

Fig. 7 XPS spectra of the catalysts

2.6 TOF

Two methods were used to prove the effect of preparation routes. The effects of different precursors on the properties of the catalysts are listed in Table 1. The particle size based on the TEM results is inconsistent with that based on the CO chemisorption results. This inconsistency can be ascribed to the partial coverage of the Ru surface by the additives. The Ru surfaces covered by promoters resulted in a lower Ru dispersion based on a lower CO absorbance. Compared with the catalyst prepared by the Ru-GLY precursor, the CO absorbance of the Ru/AC catalyst prepared with $RuCl_3$ as precursor is smaller, and the size distribution of Ru is more uneven. The activity of the catalysts prepared by co-impregnation was remarkably higher than that of the catalysts prepared by hydrogen reduction. The dispersion of Ru initially increased and then decreased with Ba content for the catalysts prepared by co-impregnation. However, their TOF values were almost the same at different Ru dispersions for the Ru+Ba6+K/AC and Ru+Ba8+K/AC catalysts. The highest TOF of the Ru+Ba12+K/AC catalyst was 1.30 s^{-1}, although the value from the Ru dispersion was almost the same as that of the Ru+Ba6+K/AC catalyst.

The catalyst with the highest activityis different from the one with the highest TOF value. The performance is closely related to the preparation methods and the promoter content of the catalysts. Co-impregnation remarkably improves the activity and TOF of the catalysts compared with conventional impregnation.

Table 1 Effect of content of different precursors on the properties of catalysts

Catalyst	Dispersion/%		Diameter/nm		NH_3 /(vol %)[a]	TOF /(S^{-1})
	d1	d2	D1	D2		
Ru-Ba10-K/AC[b]	15.6	14.7	7.1	7.5	14.20	0.69
Ru+Ba6+K/AC	11.9	10.7	9.3	10.4	15.49	0.99
Ru+Ba8+K/AC	15.6	14.5	7.1	7.6	20.28	0.99
Ru+Ba10+K/AC	17.0	16.1	6.5	6.9	19.42	0.87
Ru+Ba12+K/AC	10.8	10.1	10.2	11.0	18.49	1.30

a. Measured at 10 MPa and 10,000 h^{-1}, H_2 : N_2 = 3 : 1; Experimental error of activity of ammonia synthesis is ca. 0.2 vol%;

b. $RuCl_3$ as precursor;

d1, d2: Ru dispersion of catalysts prior and post the heat resistance, respectively;

D1, D2: Particle size of Ru based on CO chemisorption prior and post the heat resistance, respectively

2.7 Thermal stability of catalysts

The stability of the catalysts is crucial in applications. However, the methane produced during the reaction could possibly alter the structure of the catalysts, thereby decreasing the catalytic activity[35-36]. Heat treatment under the conditions of 475 ℃, 10,000 h^{-1}, and 10 MPa for 40 h can only slightly influence the activity of both Ru-Ba10-K/AC and Ru+Ba+K/AC catalysts (Table 2). This result can be related to inferior treatment temperature and short processing time. However, the activity of the Ru-Ba10-K/AC catalyst is lower than that of the Ru+Ba+K/AC, which is disadvantageous for industrial application. Therefore, the co-impregnation of promoters and precursor in the Ru/AC catalyst for ammonia synthesis is an attractive substitute for conventional impregnation. Future studies should determine the difference in stability between the two catalysts.

Table 2 Thermal stability of catalysts

Catalysts	Initial NH_3 /(vol %)	Terminational NH_3[c] /(vol %)
Ru-Ba10-K/AC[b]	14.20	14.81
Ru+Ba6+K/AC	15.49	15.21
Ru+Ba8+K/AC	20.28	20.39
Ru+Ba10+K/AC	19.42	19.64
Ru+Ba12+K/AC	18.49	18.93

a. Measured at 10 MPa and 10,000 h^{-1}, 400 ℃, H_2 : N_2 = 3 : 1;

b. $RuCl_3$ as precursor;

c. Treatment conditions: 475 ℃, 40 h, 10 000 h^{-1}, 10 MPa, H_2 : N_2 = 3 : 1;

d. Experimental error of activity of ammonia synthesis is ca. 0.2 vol%.

3 Conclusions

A co-impregnation method was used to prepare efficient catalysts for ammonia synthesis. Compared with the Ru-Ba-K/AC catalysts, the TOF significantly increased via co-impregnation. The catalysts prepared by co-impregnation have higher absorbance and lower activation energy of nitrogen based on well-defined crystal planes and the narrow size distribution of Ru NCs. The method proposed in this study allows the facile preparation of Ru nanocatalysts with high catalytic activity and high TOF based on the Ru powder predecessor.

References:

[1] Bernas A, Kumar N, Laukkanen P, *et al.* Influence of ruthenium precursor on catalytic activity of Ru/Al_2O_3 catalyst in selective isomerization of linoleic acid to cis-9, trans-11- and trans-10, cis-12-conjugated linoleic acid[J]. *Appl Catal A: Gen*, 2004, **267**: 121-133.

[2] Miyazawa T, Koso S, Kunimori K, *et al.* Development of a Ru/C catalyst for glycerol hydrogenolysis in combination with an ion-exchange resin [J]. *Appl Catal A: Gen*, 2007, **318**: 244-251.

[3] Miyazawa T, Kusunoki Y, Kunimori K, *et al.* Glycerol conversion in the aqueous solution under hydrogen over Ru/C+ an ion-exchange resin and its reaction mechanism [J]. *J Catal*, 2006, **240**: 213-221.

[4] Maris E P, Davis R J. Hydrogenolysis of glycerol over carbon-supported Ru and Pt catalysts [J]. *J Catal*, 2007, **249**: 328-337.

[5] a. Nurunnabi M, Murata K, Okabe K, *et al.* Effect of Mn addition on activity and resistance to catalyst deactivation for Fischer-Tropsch synthesis over Ru/Al_2O_3 and Ru/SiO_2 catalysts [J]. *Catal Commun*, 2007, **8**: 1531-1537.

b. Zhang Y. The performance of RuB-PEG catalyst for the hydrogenation of quinoline[J]. *J Mol Catal(China)* (分子催化), 2011, **25**(1): 37-42.

c. Li G, Dong P, Wang X, *et al.* Study of catalytic hydrogenation of 1,4-benzenediol over Ru/HY catalyst[J]. *J Mol Catal(China)*(分子催化), 2012, **26**(1): 26-31.

[6] Nurunnabi M, Murata K, Okabe K, *et al.* Performance and characterization of Ru/Al_2O_3 and Ru/SiO_2 catalysts modified with Mn for Fischer-Tropsch synthesis [J]. *Appl Catal A: Gen*, 2008, **340**: 203-211.

[7] Radkevich V Z, Senko T L, Wilson K, *et al.* The influence of surface functionalization of activated carbon on palladium dispersion and catalytic activity in hydrogen oxidation [J]. *Appl Catal A: Gen*, 2008, **335**: 241-251.

[8] a. Zhong Z H, Aika K. Effect of ruthenium precursor on hydrogen-treated active carbon supported ruthenium catalysts for ammonia synthesis [J]. *Inorg Chim Acta*, 1998, **280**: 183-188.

b. Yang X, Tang L, Xia C, *et al.* Effect of different supports on phyzical and chemical properties and catalytic activity over Ba-Ru/Mgo ammonia synthesis catalyst[J]. *J Mol Catal(China)*(分子催化), 2012, **26**(1): 1-9.

[9] a. Hinrichsen O, Rosowski F, Hornung A, *et al.* The kine- tics of ammonia synthesis over Ru-based catalysts . 1. The dissociative chemisorption and associative desorption of N_2[J]. *J Catal*, 1997, **165**: 33-44.

b. Ni J, Liu B, Zhu Y, *et al.* Effects of dual structure promoters on Ru/C catalyst for ammonia synthesis[J]. *J Mol Catal(China)*(分子催化), 2012, **27**(4): 371-376.

[10] Dahl S, Logadottir A, Jacobsen C J H, *et al.* Electronic factors in catalysis: the volcano curve and the effect of promotion in catalytic ammonia synthesis [J]. *Appl Catal A: Gen*, 2001, **222**: 19-29.

[11] Zeng H S, Inazu K, Aika K. Dechlorination process of active carbon-supported, barium nitrate-promoted ruthenium trichloride catalyst for ammonia synthesis [J]. *Appl Catal A: Gen*, 2001, **219**: 235-247.

[12] Jacobsen C J H, Dahl S, Hansen P L, *et al.* Structure sensitivity of supported ruthenium catalysts for ammonia synthesis [J]. *J Mol Catal A: Chem*, 2000, **163**: 19-26.

[13] Guraya M, Sprenger S, Rarog-Pilecka W, *et al.* The effect of promoters on the electronic structure of ruthenium catalysts supported on carbon [J]. *Appl Surf Sci*, 2004, **238**: 77-81.

[14] Rosowski F, Hornung A, Hinrichsen O, *et al.* Ruthenium catalysts for ammonia synthesis at high pressures: Preparation, characterization, and power-law kinetics [J]. *Appl Catal A: Gen*, 1997, **151**: 443-460.

[15] Schlögl R, Abd Hamid S B. Nanocatalysis: Mature Science Revisited or Something Really New? [J]. *Angew Chem Int Ed*, 2004, **43**: 1628-1637.

[16] Zhou K, Li Y. Catalysis Based on Nanocrystals with Well-Defined Facets [J]. *Angew Chem Int Ed*, 2011, **50**: 2-14.

[17] Kowalczyk Z, Krukowski M, Rarog-Pilecka W, *et al.* Carbon-based ruthenium catalyst for ammonia synthesis - Role of the barium and caesium promoters and carbon support [J]. *Appl Catal A: Gen*, 2003, **248**: 67-73.

[18] You Z, Inazu K, Aika K, *et al.* Electronic and structural promotion of barium hexaaluminate as a ruthenium catalyst support for ammonia synthesis [J]. *J Catal*, 2007, **251**: 321-331.

[19] Lin B, Wang R, Lin J, *et al.* Preparation of chlorine-free alumina-supported ruthenium catalyst for ammonia synthesis base on $RuCl_3$ by hydrazine reduction [J]. *Catal Commun*, 2007, **8**: 1838-1842.

[20] Li Y, Pan C, Han W, *et al.* An efficient route for the preparation of activated carbon supported ruthenium catalysts with high performance for ammonia synthesis [J]. *Catal Today*, 2011, **174**: 97-105.

[21] Liang C H, Wei Z B, Xin Q, *et al.* Ammonia synthesis over Ru/C catalysts with different carbon supports promoted by barium and potassium compounds [J]. *Appl Catal A: Gen*, 2001, **208**: 193-201.

[22] Asscher M, Carrazza J, Khan M M, *et al.* The ammonia

synthesis over rhenium single-crystal catalysts: Kinetics, structure sensitivity, and effect of potassium and oxygen [J]. *J Catal*, 1986, **98**: 277-287.

[23] Kowalczyk Z, Krukowski M, Rarog-Pilecka W, *et al.* Carbon-based ruthenium catalyst for ammonia synthesis - Role of the barium and caesium promoters and carbon support [J]. *Appl Catal A: Gen*, 2003, **248**: 67-73.

[24] Zhang L, Lin J, Ni J, *et al.* Highly efficient Ru/Sm_2O_3-CeO_2 catalyst for ammonia synthesis [J]. *Catal Commun*, 2011, **15**: 23-26.

[25] Aika K, Kubota J, Kadowaki Y, *et al.* Molecular sensing techniques for the characterization and design of new ammonia catalysts [J]. *Appl Surf Sci*, 1997, **121**: 488-491.

[26] Rarog-Pilecka W, Szmigiel D, Kowalczyk Z, *et al.* Ammonia decomposition over the carbon-based ruthenium catalyst promoted with barium or cesium [J]. *J Catal*, 2003, **218**: 465-469.

[27] Wang X, Ni J, Lin B, *et al.* Highly efficient Ru/MgO-CeO_2 catalyst for ammonia synthesis [J]. *Catal Commun*, 2010, **12**: 251-254.

[28] Spencer N D, Schoonmaker R C, Somorjai G A. Iron single crystals as ammonia synthesis catalysts: Effect of surface structure on catalyst activity [J]. *J Catal*, 1982, **74**: 129-135.

[29] Somorjai G, Materer N. Surface structures in ammonia synthesis [J]. *Top Catal*, 1994, **1**: 215-231.

[30] Ramos-Fernández E V, Silvestre-Albero J, Sepúlveda-Escribano A, *et al.* Effect of the metal precursor on the properties of Ru/ZnO catalysts [J]. *Appl Catal A: Gen*, 2010, **374**: 221-227.

[31] Nachimuthu P, Kim Y J, Kuchibhatla S V N T, *et al.* Growth and characterization of barium oxide nanoclusters on YSZ(111) [J]. *The Journal of Physical Chemistry C*, 2009, **113**: 14324-14328.

[32] Paik U, Yeo J-G, Lee M-H, *et al.* Dissolution and re-precipitation of barium at the particulate $BaTiO_3$-aqueous solution interface [J]. *Mater Res Bull*, 2002, **37**: 1623-1631.

[33] Hansen T W, Wagner J B, Hansen P L, *et al.* Atomic-resolution in situ transmission electron microscopy of a promoter of a heterogeneous catalyst [J]. *Science*, 2001, **294**: 1508-1510.

[34] Truszkiewicz E, Raróg-Pilecka W, Schmidt-Szalowski K, *et al.* Barium-promoted Ru/carbon catalyst for ammonia synthesis: State of the system when operating [J]. *J Catal*, 2009, **265**: 181-190.

[35] Rossetti I, Mangiarini F, Forni L. Promoters state and catalyst activation during ammonia synthesis over Ru/C [J]. *Appl Catal A: Gen*, 2007, **323**: 219-225.

[36] Zheng X L, Zhang S J, Xu J X, *et al.* Effect of thermal and oxidative treatments of activated carbon on its surface structure and suitability as a support for barium-promoted ruthenium in ammonia synthesis catalysts [J]. *Carbon*, 2002, **40**: 2597-2603.

共浸渍制备高效的 Ru/AC 氨合成催化剂

倪 军*, 朱永龙, 陈 赓, 林建新, 魏可镁

(福州大学 化肥催化剂国家工程研究中心, 福建 福州 350002)

摘要: 通过钌的配合物前驱体和硝酸钡的共浸渍制备的 Ru+Ba+K/AC 催化剂氨合成转化效率高, 其氨合成转化频率在 0.87 ~ 1.30 s^{-1} 之间, 与氯化钌制备的 Ru/AC 催化剂相比, 其转化频率提高幅度在 26% ~ 88%. 共浸渍法制备的催化剂氨合成转化效率高, 其主要原因可能是共浸渍法制备的催化剂钌粒子粒径分布区间较窄, 易形成更多的活性位; 钌表面氢的吸附受到抑制, 氮更易活化, 因而催化效率更高.

关键词: 钌; 负载型催化剂; 多相催化; 共浸渍; 转化频率